

High Pressure Oxidation of Dimethoxymethane

Lorena Marrodán, Eduardo Royo, Ángela Millera, Rafael Bilbao, and María U. Alzueta*

Aragón Institute of Engineering Research (I3A), Department of Chemical and Environmental Engineering, University of Zaragoza, 50018 Zaragoza, Spain

S Supporting Information

ABSTRACT: The oxidation of dimethoxymethane (DMM) has been studied under a wide range of temperatures (373–1073 K), pressures (20–60 bar) and air excess ratios ($\lambda = 0.7, 1$ and 20), from both experimental and modeling points of view. Experimental results have been interpreted and analyzed in terms of a detailed gas-phase chemical kinetic mechanism for describing the DMM oxidation. The results show that the DMM oxidation regime for 20, 40 and 60 bar is very similar for both reducing and stoichiometric conditions. For oxidizing conditions, a plateau in the DMM, CO and CO₂ concentration profiles as a function of the temperature can be observed. This zone seems to be associated with the peroxy intermediate, CH₃OCH₂O₂, whose formation and consumption reactions appear to be important for the description of DMM conversion under high pressure and high oxygen concentration conditions.

INTRODUCTION

Diesel engines are used for transportation because of their high fuel efficiency. However, they highly contribute to nitrogen oxides (NO_x) and particulate matter (PM) emissions, which are difficult to reduce simultaneously in conventional diesel engines (NO_x formation is favored under fuel-lean conditions, whereas PM is formed when there is a lack of oxygen). The addition of oxygenated compounds to diesel fuel can effectively reduce these emissions.^{1–4} For instance, the reduction of smoke has been reported to be strongly related to the oxygen content of blends⁵ without increasing the NO_x and engine thermal efficiency.

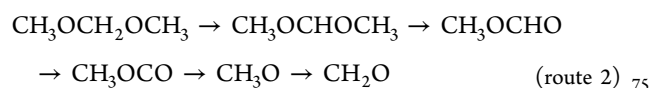
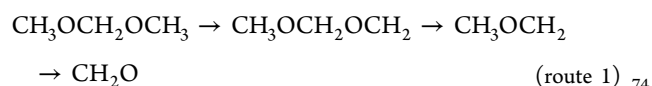
Dimethoxymethane (methylal or DMM, CH₃OCH₂OCH₃) is a diether considered to be a potential fuel additive. In comparison to the simplest ether, dimethyl ether (DME), which has been widely proposed and tested for using with diesel fuel as a means of reducing exhaust emissions,^{6,7} DMM has a higher quantity of oxygen, lower vapor pressure and better solubility with diesel fuel. Several studies have analyzed the effect of adding DMM to base diesel on emissions of compression ignition engines or direct injection engines (e.g., Ren et al.⁸) and, in general, diesel–DMM blends increase engine performance and decrease exhaust emissions.

Huang et al.⁹ studied the combustion and the emissions of a compression ignition engine fuelled with blends of diesel–DMM. They found that a remarkable reduction in the exhaust CO and smoke can be achieved when operating with diesel–DMM blends, and a simultaneous reduction in both NO_x and smoke can be obtained with large DMM additions. Sathiyaganam and Saravanan¹⁰ also analyzed the effects of DMM addition to diesel, and obtained an appreciable reduction of emissions such as smoke density, particulate matter and a marginal increase in the performance when compared with the normal diesel run. Chen et al.¹¹ developed an experimental and modeling study of the effects of adding oxygenated fuels to premixed *n*-heptane flames and found that, as oxygenated fuels were added, mole fractions of most C₁–C₅ hydrocarbon

intermediates were significantly reduced together with an apparent decrease of benzene amount.

Although a great volume of experiments have been conducted to determine the effects of diesel–DMM blends on the CO and smoke emissions, few studies have been focused on the combustion characteristics of pure DMM fuel at high temperatures¹² and even less at high pressures.

Daly et al.¹³ investigated the oxidation of DMM in a jet-stirred reactor at a pressure of 5.07 bar, high temperatures of 800–1200 K and equivalence ratios of 0.444 ($\lambda = 2.25$), 0.889 ($\lambda = 1.13$) and 1.778 ($\lambda = 0.56$), and proposed a submechanism of 50 reactions relevant to describe the combustion of DMM, including a significant number of estimated rate constants. Recently, Dias et al.¹⁴ have studied lean and rich premixed DMM flames to build a submechanism taking into account the formation and the consumption of oxygenated species involved in DMM oxidation. They were able to build a new mechanism containing 480 elementary reactions and involving 90 chemical species, by using kinetic data from the literature about DMM, mainly drawn from Daly et al.,¹³ in order to simulate the DMM flames. Whatever the availability of oxygen in the flow, they established two main DMM conversion routes, with the first one being the fastest:



In this context, a study on DMM oxidation carried out under well controlled tubular flow reactor conditions at atmospheric pressure, from pyrolysis to high oxidizing conditions, from both

Received: March 3, 2015

Revised: April 22, 2015

79 experimental and modeling points of view, was previously
80 developed by our research group.¹⁵ The results obtained
81 indicate that the initial oxygen concentration slightly influences
82 the consumption of DMM. In general, a good agreement
83 between experimental and modeling data was obtained and,
84 accordingly, the final mechanism compiled in that work has
85 been taken as the initial mechanism in the present work.

86 Therefore, the purpose of the present work is to carry out an
87 experimental study of DMM conversion at high pressure
88 covering a large range of temperature, pressure and different
89 stoichiometries, together with the validation of a kinetic
90 mechanism under high-pressure conditions, which would be
91 of interest for diesel applications. Specifically, experiments have
92 been performed under well-controlled flow reactor conditions,
93 in the 373–1073 K temperature range and for different high
94 pressures (20, 40 and 60 bar). Under these conditions, the
95 oxygen concentration was varied from 1960 to 56 000 ppm,
96 resulting in different air excess ratios (λ) ranging from 0.7 to 20.
97 Additionally, a modeling study to describe the oxidation of
98 DMM was performed using the gas-phase detailed chemical
99 kinetic mechanism of our previous work,¹⁵ which has been
100 updated in the present work to account for working at high
101 pressures.

102 ■ EXPERIMENTAL SECTION

103 The experimental installation used in the present work is described in
104 detail elsewhere,¹⁶ and only a brief description is given here. It consists
105 basically of a gas feeding system, a reaction system and a gas analysis
106 system.

107 Gases are supplied from gas cylinders through mass flow controllers.
108 A concentration of approximately 700 ppm of DMM is introduced in
109 all the experiments. The amount of O₂ used has been varied between
110 1960 and 56 000 ppm, and is related to the air excess ratio (λ), defined
111 as the inlet oxygen concentration divided by the stoichiometric
112 oxygen. Therefore, values of λ lower than 1 refer to fuel rich
113 conditions, and λ values larger than 1, refer to fuel lean conditions.
114 Nitrogen is used to balance, resulting in a constant flow rate of 1000
115 (STP) mL/min.

116 The DMM oxidation takes place in a quartz flow reactor (inner
117 diameter of 6 mm and 1500 mm in length) that is enclosed in a
118 stainless steel tube that acts as a pressure shell. Nitrogen is delivered to
119 the shell side of the reactor by a pressure control system, to obtain a
120 pressure similar to that inside the reactor avoiding this way the stress
121 in the reactor.

122 The reactor tube is placed horizontally in a three-zone electrically
123 heated furnace, ensuring a uniform temperature profile within ± 10 K
124 throughout the isothermal reaction zone (56 cm). The gas residence
125 time, t_r , in the isothermal zone, is a function of the reaction
126 temperature and pressure, t_r (s) = $261 \cdot P$ (bar)/ T (K).

127 Downstream the reactor, the pressure is reduced to atmospheric
128 level. Before analysis, the product gases pass through a condenser and
129 a filter to ensure gas cleaning. The outlet gas composition is measured
130 using a gas micro chromatograph (Agilent 3000), which is able to
131 detect and measure DMM and the main products of its oxidation:
132 methyl formate (CH₃OCHO), formaldehyde (CH₂O), CO, CO₂ and
133 CH₄. No other products were detected in a noticeable amount. The
134 uncertainty of measurements is estimated as $\pm 5\%$. To evaluate the
135 goodness of the experiments, the atomic carbon balance was checked
136 in all the experiments and resulted to close always near 100%.

137 The experiments were carried out at different pressures (20, 40 and
138 60 bar) and in the 373–1073 K temperature range. Table 1 lists the
139 conditions of the experiments.

140 ■ MODELING

141 The experimental results have been analyzed in terms of a
142 detailed gas-phase chemical kinetic mechanism for describing

Table 1. Matrix of Experimental Conditions^a

exp.	DMM (ppm)	O ₂ (ppm)	λ	P (bar)
set 1	720	1960	0.7	20
set 2	770	1960	0.7	40
set 3	770	1960	0.7	60
set 4	757	2800	1	20
set 5	720	2800	1	40
set 6	720	2800	1	60
set 7	688	56000	20	20
set 8	778	56000	20	40
set 9	706	56000	20	60

^aThe experiments are conducted at constant flow rate of 1000 mL (STP)/min, in the temperature interval of 373–1073 K. The balance is closed with N₂. The residence time depends on the reaction temperature and pressure: t_r (s) = $261 \cdot P$ (bar)/ T (K).

the oxidation of DMM. The model taken as starting point was
the kinetic mechanism compiled in the previously appointed
work about the DMM oxidation at atmospheric pressure by our
research group.¹⁵ This one was built by adding different
reaction subsets found in the literature to the model developed
by Glarborg et al.¹⁷ updated and extended later.^{18,19} The
additional reaction subsets included for the different expected
or involved compounds of relevance for the present experi-
ments were dimethyl ether (DME),²⁰ ethanol,²¹ acetylene²²
and methyl formate (MF).²³ The last subset was revised by our
group¹⁶ to account for high-pressure conditions in the methyl
formate oxidation, which are similar to those of the present
work. For DMM, the Dias et al. reaction subset¹⁴ developed for
atmospheric pressure was also included. Thermodynamic data
for the involved species are taken from the same sources as the
cited mechanisms.

The model used in the previous work¹⁵ has been modified in
the present work to account also for the high-pressure
conditions studied in the DMM oxidation. The changes made
to the mechanism are listed in Table 2 and will be described
below. The final mechanism involves 726 reactions and 142
species.

Thermal decomposition of DMM is an important initiation
step, and can occur through DMM breaking, reactions route 1
and route 2, or by losing a primary or a secondary hydrogen
atom, reactions 3 and 4, respectively. The constants for these
reactions were kept, without any modification, from the work of
Dias et al.,¹⁴ originally proposed by Daly et al.¹³

For reaction route 1, the value of $2.62 \times 10^{16} \exp(-41\,369/T)$
cm³ mol⁻¹ s⁻¹ for the rate constant was taken from the
estimation made by Dagaut et al.²⁴ for DME, from a fit of the
available NIST²⁵ data. For reaction route 2, the value for the
rate constant, $2.51 \times 10^{15} \exp(-38\,651/T)$ cm³ mol⁻¹ s⁻¹,
estimated by Foucaut and Martin by analogy with diethyl
ether²⁶ was taken, and for reaction 3, the kinetic parameters
($4.35 \times 10^{16} \exp(-50\,327/T)$ cm³ mol⁻¹ s⁻¹) were taken from
the estimation for the similar reaction involving ethane.²⁷
Finally, for the loss of a secondary hydrogen atom from DMM,
reaction 4, Dean²⁷ estimated the rate constant by analogy with
the rate constant for the loss of a secondary atom of hydrogen
from propane, with a value of $6.31 \times 10^{15} \exp(-47\,660/T)$ cm³
mol⁻¹ s⁻¹.

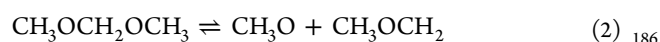
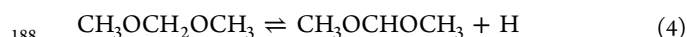
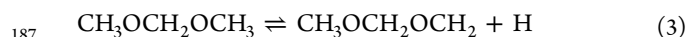


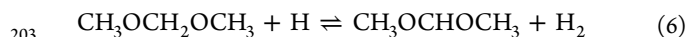
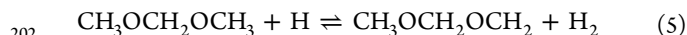
Table 2. Reactions Modified or Included in the Final Mechanism in Relation to the Mechanism Used in Reference 15 and Corresponding Kinetic Parameters^a

number	reaction	A	n	E _a	source
9	CH ₃ OCH ₂ OCH ₃ + OH ⇌ CH ₃ OCH ₂ OCH ₂ + H ₂ O	6.32 × 10 ⁶	2.00	-652	[refs 22, 32 and 34, see text]
10	CH ₃ OCH ₂ OCH ₃ + OH ⇌ CH ₃ OCHOCH ₃ + H ₂ O	6.32 × 10 ⁶	2.00	-652	[refs 22, 32 and 34, see text]
11	CH ₃ OCH ₂ OCH ₃ + HO ₂ ⇌ CH ₃ OCH ₂ OCH ₂ + H ₂ O ₂	1.00 × 10 ¹³	0.00	17686	35
12	CH ₃ OCH ₂ OCH ₃ + HO ₂ ⇌ CH ₃ OCHOCH ₃ + H ₂ O ₂	2.00 × 10 ¹²	0.00	15296	13
15	CH ₃ OCH ₂ OCH ₂ + O ₂ ⇌ CH ₂ O + CH ₃ OCHO + OH	2.50 × 10 ¹¹	0.00	-1700	22
16	CH ₃ OCHOCH ₃ + O ₂ ⇌ CH ₂ O + CH ₃ OCHO + OH	2.50 × 10 ¹¹	0.00	-1700	22
17	CH ₃ OCH ₂ OCH ₂ + HO ₂ ⇌ CH ₂ O + CH ₃ OCH ₂ O + OH	3.00 × 10 ¹¹	0.00	0	13
18	CH ₃ OCHOCH ₃ + HO ₂ ⇌ CH ₃ OCHO + CH ₃ O + OH	1.00 × 10 ¹²	0.00	0	13
19	CH ₃ OCH ₂ OCH ₂ + O ₂ ⇌ CH ₃ OCH ₂ O ₂ + CH ₂ O	6.40 × 10 ¹²	0.00	91	see text
20	CH ₃ OCH ₂ OCH ₂ + HO ₂ ⇌ CH ₃ OCH ₂ O ₂ + CH ₂ OH	1.00 × 10 ¹²	0.00	0	see text

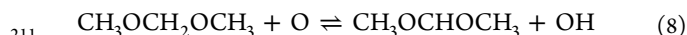
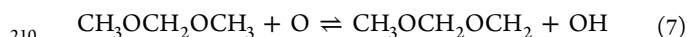
^aA is in cm³ mol⁻¹ s⁻¹; E_a is in cal/mol.



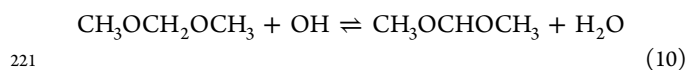
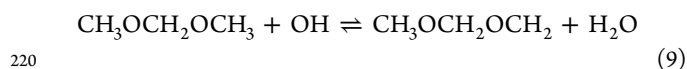
189 An important pathway for DMM consumption includes
 190 hydrogen abstraction reactions by the O/H radical pool. For
 191 the reactions with H (reactions 5 and 6), the rate expressions
 192 were taken from the DMM subset proposed by Dias et al.,¹⁴
 193 which were, a priori, taken from Daly et al.¹³ The rate constant
 194 of reaction 5 was taken as that for the reaction between DME
 195 and a hydrogen atom,²⁸ that is 9.70 × 10¹³ exp(-3125/T) cm³
 196 mol⁻¹ s⁻¹. For reaction 6, the 7.40 × 10¹² exp(-1631/T) cm³
 197 mol⁻¹ s⁻¹ rate constant was based on the abstraction of a
 198 secondary hydrogen atom from diethyl ether.²⁹ Although, Dias
 199 et al.¹⁴ included an A-factor for this reaction divided by 2 in
 200 their final mechanism, we adopted the value originally proposed
 201 by Daly et al.,¹³ which is 7.40 × 10¹² cm³ mol⁻¹ s⁻¹.



204 In the case of the reactions between DMM and O radicals
 205 (reactions 7 and 8), their rate constants were taken from the
 206 DMM subset proposed by Dias et al.¹⁴ without any
 207 modification, previously adopted from,³⁰ by analogy with
 208 CH₃OCH₂ for reaction 7, and by analogy with diethyl ether,
 209 for reaction 8.



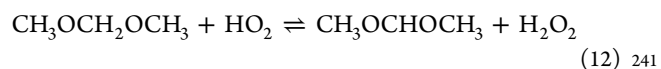
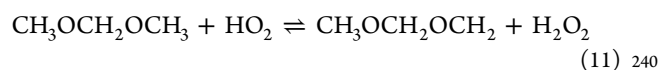
212 Reaction with hydroxyl radicals (OH) is an important step in
 213 the oxidation of organic compounds in combustion systems.³¹
 214 Although it will be discussed later through the analysis of the
 215 different reaction pathways, the main consumption of DMM
 216 occurs through H abstraction reactions by OH to form
 217 CH₃OCH₂OCH₂ and CH₃OCHOCH₃ radicals (reactions 9
 218 and 10). The kinetic parameters of these reactions have been
 219 modified from the previous work.¹⁵



222 In the Dias et al. DMM reaction subset,¹⁴ the rate constant of
 223 these reactions is estimated by analogy with the reaction
 224 CH₃OCH₃ + OH ⇌ CH₃OCH₂ + H₂O from DeMore and
 225 Bayes,³² with a proposed value of 9.10 × 10¹² exp(-496/T)

cm³ mol⁻¹ s⁻¹, determined experimentally in the 263–361 K 226
 temperature range. Arif et al.³¹ determined a rate constant of 227
 6.32 × 10⁶ T² exp(327/T) cm³ mol⁻¹ s⁻¹, in the 295–650 K 228
 temperature range, which is adopted in this study, also used in 229
 the work of Alzueta et al.,²⁰ and that is in agreement with the 230
 high-temperature (923–1423 K) determination of Cook et al.³³ 231
 With this value, the latest authors achieved a good fit for both 232
 the low and the high temperature measurements. 233

The prevalence of HO₂ radicals under high pressure, and 234
 preferably lean conditions, should make them to play an 235
 important role under the conditions of the present work. 236
 Reactions involving DMM and HO₂ radicals (reactions 11 and 237
 12) were not included in the initial reaction subset of Dias et 238
 al.,¹⁴ and we have included them in the present work. 239



The rate constants for reactions 11 and 12 have not been 242
 measured to our knowledge and, therefore, there is some 243
 degree of uncertainty in their absolute values. For reaction 11, 244
 the rate parameters have been taken by analogy of the dimethyl 245
 ether and HO₂ reaction, following the same procedure 246
 described by Daly et al.,¹³ and likewise taking the value, 1.00 247
 × 10¹³ exp(-8900/T) cm³ mol⁻¹ s⁻¹, from the work of Curran 248
 et al.³⁴ The rate constant for abstraction of a secondary 249
 hydrogen atom (reaction 12) was estimated by Daly et al.¹³ 250
 from the value for reaction 11, with the A factor divided by a 251
 factor of 6. These authors stated that DMM has six primary 252
 hydrogen atoms and only two secondary ones, so the 253
 probability of attack will therefore be lower for the attack on 254
 the CH₂ groups than on the CH₃ groups. Also, the proximity of 255
 two oxygen atoms to the central carbon atom of the molecule 256
 will make the hydrogen atoms attached to it more labile than 257
 those belonging to the methyl groups. As a result, the activation 258
 energy for reaction 12 should be lower than for reaction 11. 259
 Thus, a rate constant value of 2.00 × 10¹² exp(-7698/T) cm³ 260
 mol⁻¹ s⁻¹ was proposed for reaction 12,¹³ which is adopted in 261
 the present mechanism. 262

The subset proposed by Dias et al.¹⁴ includes reactions 263
 involving DMM with molecular oxygen (reaction 13 and 14) 264
 and their corresponding rate constants, adopted here with no 265
 modification from the work of Daly et al.,¹³ were both 266
 estimated by analogy with the reaction of DME with oxygen. 267
 Therefore, the rate parameters for reaction 13 are the same as 268
 those considered by Dagaut et al.²⁴ (although for reaction 13, 269

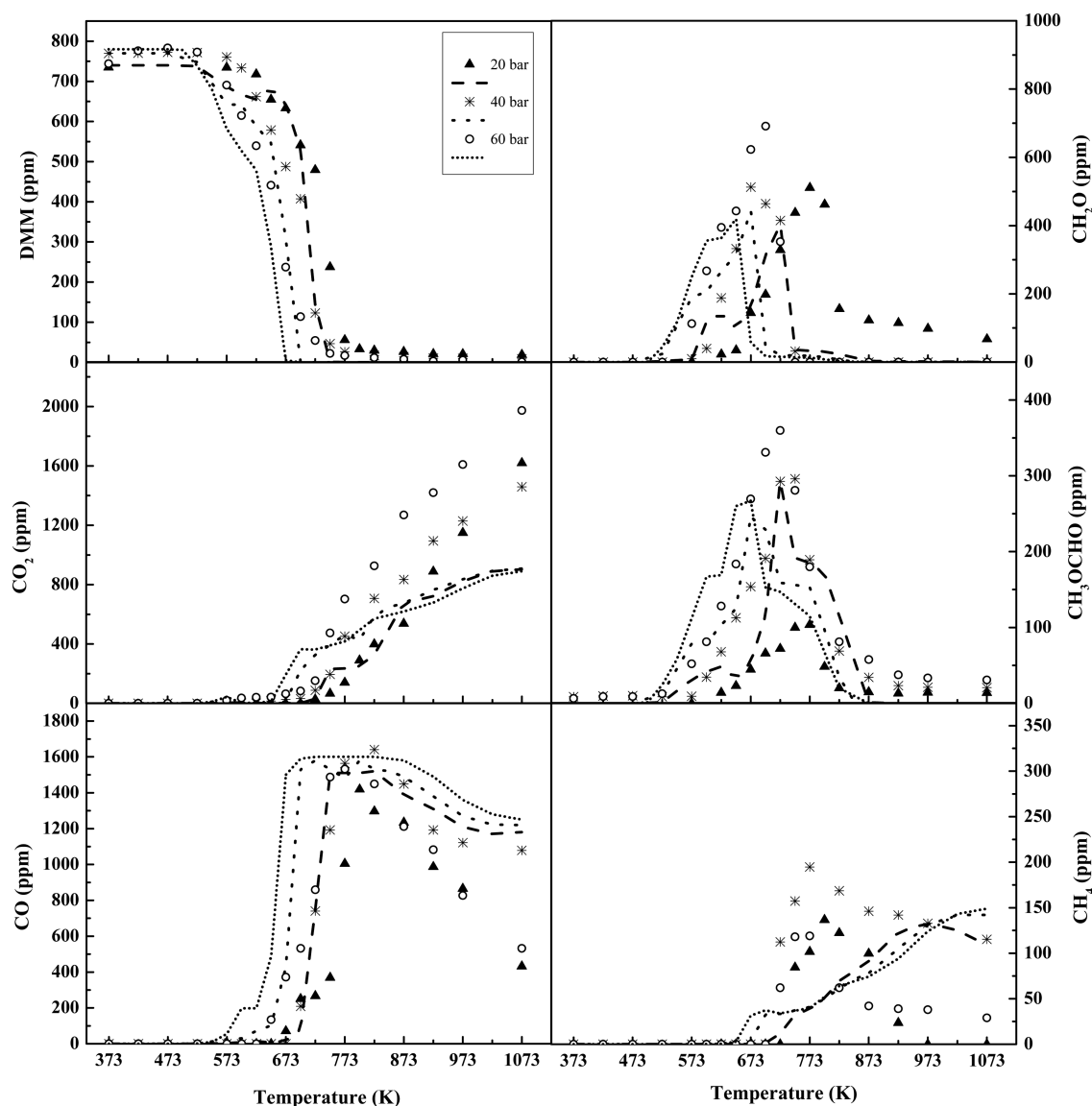
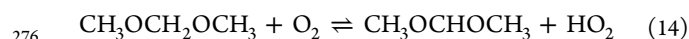
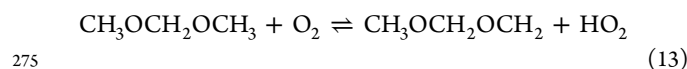
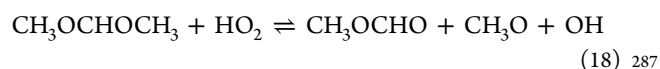
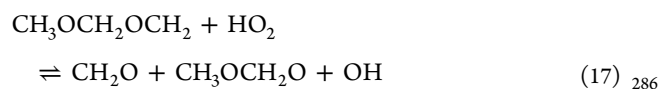
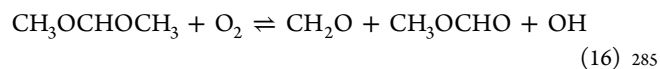
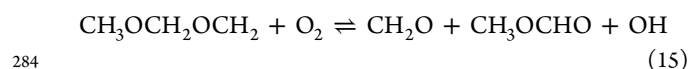


Figure 1. Influence of pressure on the DMM, CO₂, CO, CH₂O, CH₃OCHO and CH₄ concentration profiles as a function of temperature for a given air excess ratio ($\lambda = 0.7$). Sets 1–3 in Table 1.

270 the values used by Dias et al.¹⁴ are not the corresponding ones
 271 to the source specified, as also was indicated in the case of
 272 reaction 6), and the parameters for reaction 14 were estimated
 273 by Daly et al.¹³ as previously done in the case of reactions
 274 involving HO₂ radicals.



277 Although the reactions of CH₃OCH₂OCH₂ and
 278 CH₃OCHOCH₃ radicals with O₂ (reactions 15 and 16) and
 279 HO₂ (reactions 17 and 18) were omitted in previous DMM
 280 mechanisms,^{14,15,34} they can play an important role in the
 281 oxidation of DMM, particularly under high pressure and high
 282 oxygen concentration conditions and, therefore, these reactions
 283 have been included in our final mechanism.



For reactions 15 and 16, the rate constants have been 288
 estimated, establishing an analogy with the reaction of 289
 methoxy-methyl radical (CH₃OCH₂, generated in the dimethyl 290
 ether thermal decomposition) and oxygen molecular, as 291
 previously done by Daly et al.¹³ In that case, they chose the 292
 kinetic parameters given by Dagaut et al.,²⁴ namely, 1.70×10^{10} 293
 $\exp(337/T) \text{ cm}^3 \text{ mol}^{-1} \text{ s}^{-1}$, which were estimated based on 294
 C₂H₅ + O₂ kinetics. However, here, we have chosen a value of 295
 the CH₃OCH₂ + O₂ rate constant of $2.50 \times 10^{11} \exp(850/T)$ 296
 $\text{cm}^3 \text{ mol}^{-1} \text{ s}^{-1}$, obtained by Alzueta et al.²⁰ from averaging three 297
 room-temperature determinations,^{35–37} and adopting the 298
 temperature dependence reported in Hoyerann and 299

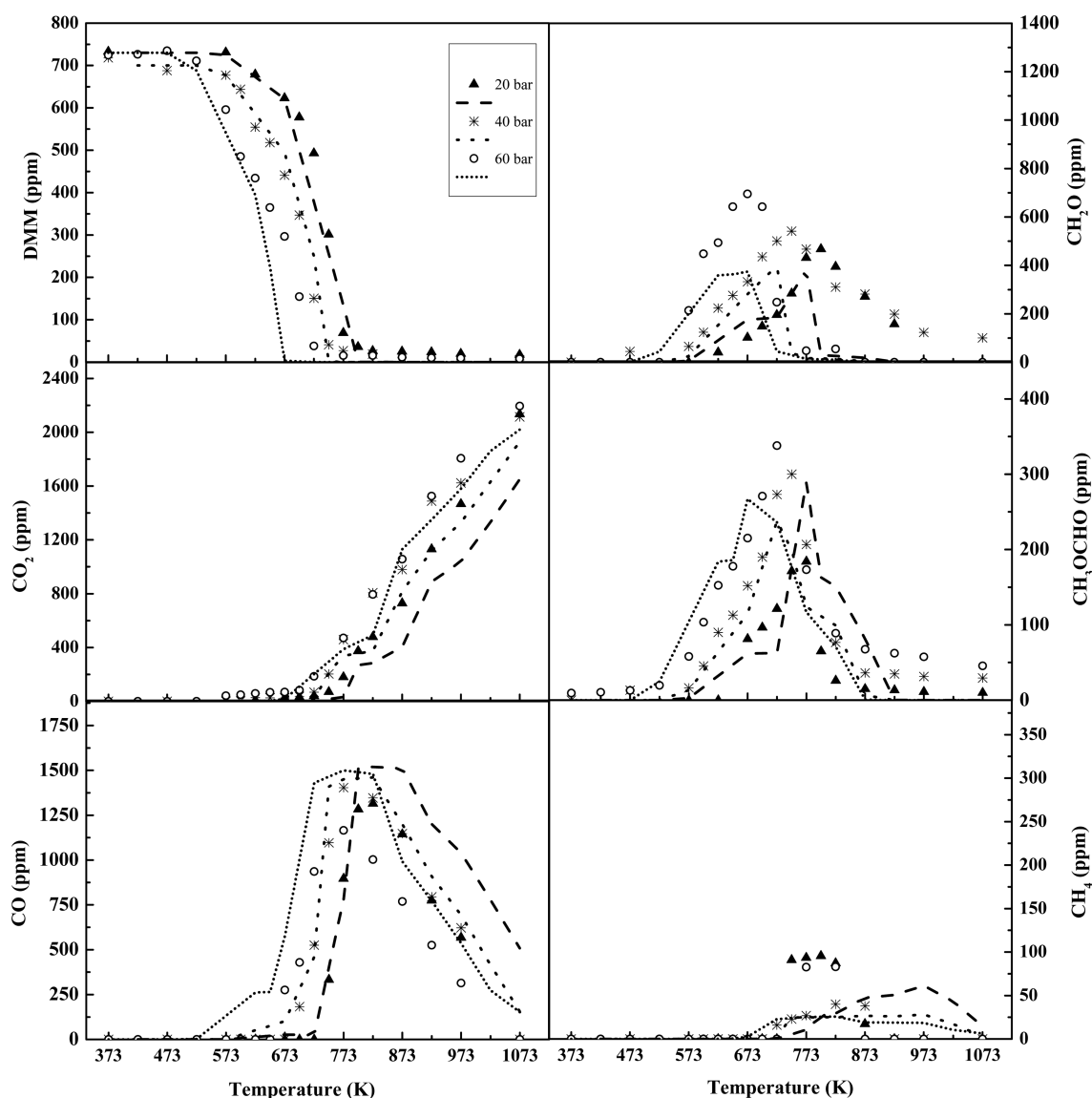


Figure 2. Influence of pressure on the DMM, CO_2 , CO, CH_2O , CH_3OCHO and CH_4 concentration profiles as a function of temperature for a given air excess ratio ($\lambda = 1$). Sets 4–6 in Table 1.

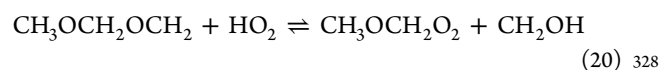
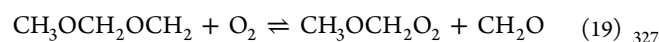
300 Nacke,³⁷ which is significantly faster than that proposed in the
301 mechanism of Dagaut et al.²⁴

302 In the same way, the analogy used before in the case of
303 reactions with molecular oxygen ($\text{CH}_3\text{OCH}_2 + \text{O}_2$) has been
304 applied to obtain the rate constants of reactions 17 and 18, i.e.,
305 $\text{CH}_3\text{OCH}_2 + \text{HO}_2$. Not much information has been found
306 related to these reactions, and the value proposed by Daly et
307 al.,¹³ based on estimations made by Dagaut et al.²⁴ has been
308 chosen. This value is, for reaction 17, $3.00 \times 10^{11} \text{ cm}^3 \text{ mol}^{-1} \text{ s}^{-1}$
309 and, for reaction 18, they increased this value to 1.00×10^{12}
310 $\text{ cm}^3 \text{ mol}^{-1} \text{ s}^{-1}$.

311 Curran et al.³⁴ stated that the pathway involving peroxy
312 intermediates may be important at low temperatures (below
313 approximately 900 K) and pressures higher than 10 bar,
314 because the bimolecular addition of methoxy-methyl radical to
315 O_2 has a lower activation energy barrier than the β -scission to
316 yield CH_2O and CH_3 , the two main pathways that methoxy-
317 methyl radicals can undergo. At atmospheric pressure (e.g.,
318 Alzueta et al.²⁰), the formation of methoxy methyl-peroxy

intermediate is not predicted to be significant, except for a
319 minor contribution for very lean stoichiometries. 320

321 Under the conditions studied in this work, high pressures
322 (20, 40 and 60 bar) and fuel lean conditions ($\lambda = 20$), the
323 reactions forming peroxy species (reactions 19 and 20) may
324 have an important impact on the oxidation chemistry of DMM
325 and, therefore, these reactions have been included in our final
326 mechanism. 326



329 For reaction 19, the kinetic parameters have been estimated
330 by analogy with the reaction of methoxy-methyl radical with
331 molecular oxygen. The $6.40 \times 10^{12} \exp(-45.80/T) \text{ cm}^3 \text{ mol}^{-1}$
332 s^{-1} value for $\text{CH}_3\text{OCH}_2 + \text{O}_2$ was considered in an earlier
333 mechanism by our group.²⁰ For reaction 20, no values of kinetic
334 parameters were found, and we have considered initially a
335 reaction rate of $1.0 \times 10^{12} \text{ cm}^3 \text{ mol}^{-1} \text{ s}^{-1}$. The results of 335

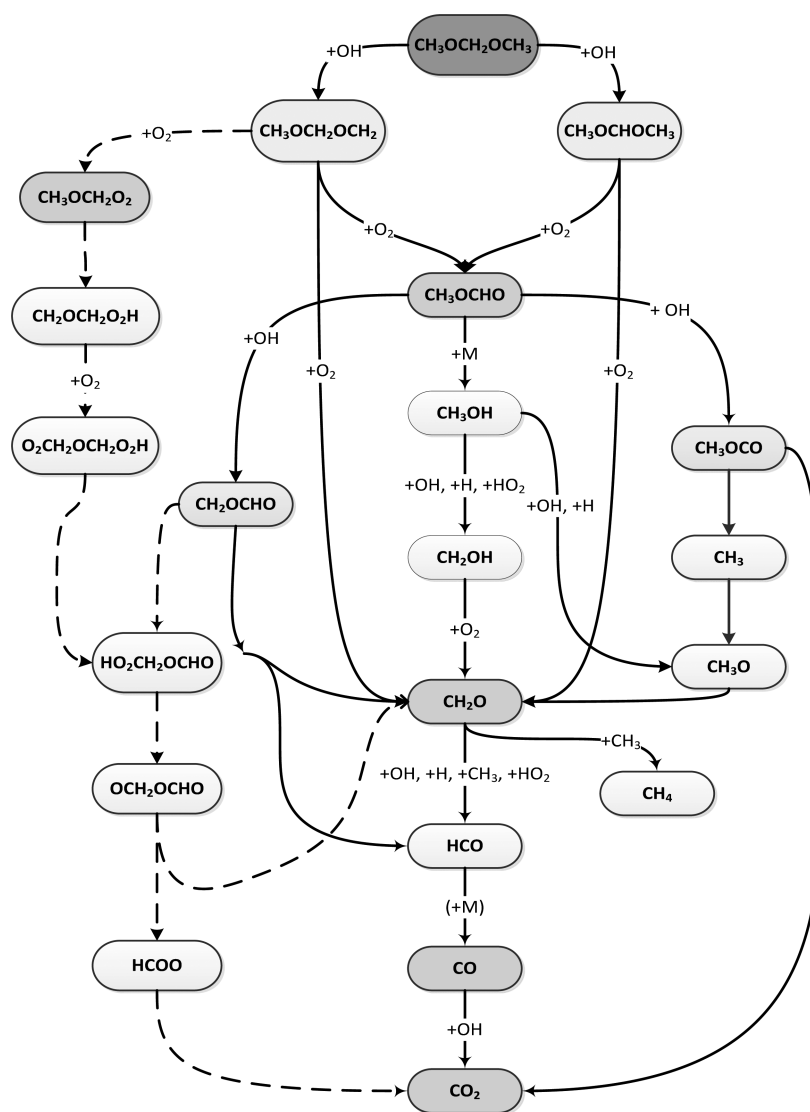


Figure 3. Reaction path diagram for DMM oxidation according to the current kinetic model in the 373–1073 K temperature range. Solid lines represent the main reaction pathways for all the conditions considered in the present work. Dashed lines refer to reaction paths that become more relevant under oxidizing conditions ($\lambda = 20$) and increasing pressure.

sensitivity analysis, shown later, indicate no significant impact of this estimation.

Model calculations have been performed using both SENKIN³⁸ from the CHEMKIN II software package³⁹ and CHEMKIN-PRO,⁴⁰ considering pressure constant in the reaction zone and the corresponding temperature profile. An example of temperature profiles inside the reactor can be found in ref 16. The full mechanism listing and thermochemistry used can be found as Supporting Information.

RESULTS AND DISCUSSION

In this work, a study of the oxidation of DMM at different pressures (20, 40 and 60 bar), and in the 373–1073 K temperature range, has been carried out. In addition to temperature and pressure, the influence of stoichiometry ($\lambda = 0.7, 1$ and 20) on the oxidation process has also been analyzed. As mentioned, the experimental results have been interpreted in terms of the detailed kinetic mechanism previously described.

Figures 1 and 2 show the influence of the temperature and pressure for specific air excess ratios, $\lambda = 0.7$ and $\lambda = 1$, respectively, on the concentration of DMM and the formation of the main products of its oxidation at high pressures: CH_2O , CO_2 , CO , CH_3OCHO and CH_4 . No other products have been detected in an appreciable amount. At atmospheric pressure, other products such as C_2H_4 , C_2H_6 and C_2H_2 , were detected through micro GC analysis in amounts lower than 100 ppm, and especially for reducing ($\lambda = 0.7$), very reducing ($\lambda = 0.4$) and pyrolysis ($\lambda = 0$) conditions.¹⁵ Methanol is highly formed at atmospheric pressure,¹⁵ while at higher pressures (20–60 bar) formaldehyde is predominant, although the distinction between methanol and formaldehyde with micro-GC techniques sometimes is quite tricky.

Both Figures 1 and 2 compare experimental (symbols) and model calculation (lines) results. Working at 20, 40 or 60 bar does not have a big effect neither on the oxidation of DMM nor on the formation of the main products. The suggested model predicts the general trend of the different concentration profiles, although there are some discrepancies between experimental and simulation results. These discrepancies are

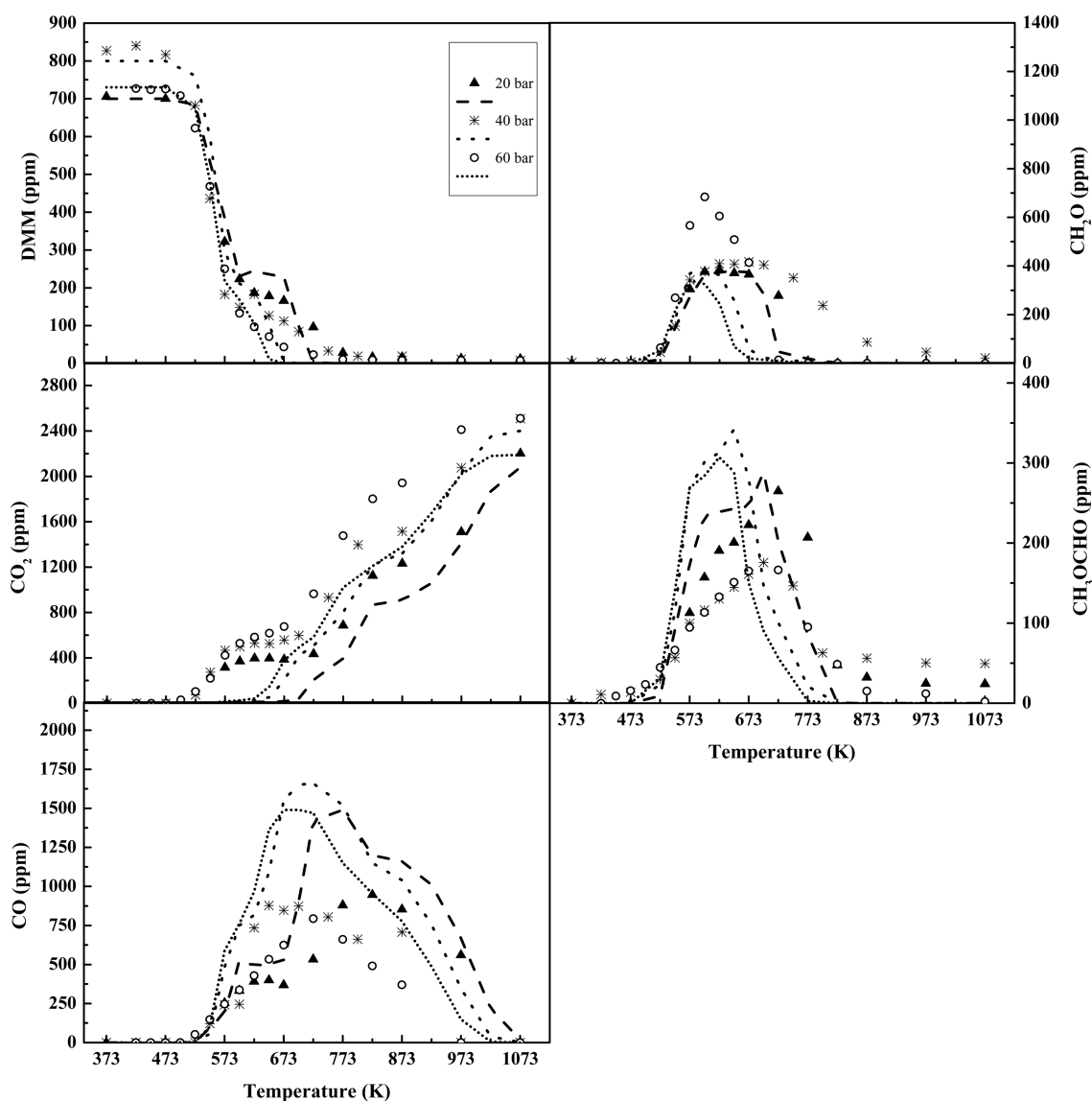


Figure 4. Influence of pressure on the DMM, CO_2 , CO, CH_2O and CH_3OCHO concentration profiles as a function of temperature for a given air excess ratio ($\lambda = 20$). Sets 7–9 in Table 1.

especially remarkable for $\lambda = 0.7$, where the CO_2 concentration values at high temperatures are underestimated, whereas the CO values are overestimated. It is difficult to isolate the origin of those discrepancies, and may be attributed to the uncertainty in the conversion of intermediates. This fact is not observed for the other values of λ considered. The oxygen concentration in the reactant mixture slightly influences the conversion of DMM, similar to what has been observed in the oxidation behavior of other oxygenated compounds such as DME²⁰ or MF.¹⁶

Figure 3 shows a reaction path diagram for DMM oxidation through a reaction rate analysis with the mechanism used in the present work. For the conditions analyzed in the present work, the main consumption of DMM is through H abstraction reactions by the hydroxyl radical (OH) to form $\text{CH}_3\text{OCH}_2\text{OCH}_2$ and $\text{CH}_3\text{OCHOCH}_3$ radicals (reactions 9 and 10), which is in agreement with other previous works.¹³ Both reactions have a relative importance of 38%. This value increases up to near 50% under oxidizing conditions.

Both radicals react with molecular oxygen to form methyl formate (CH_3OCHO) and formaldehyde as main products (reactions 15 and 16).

Formaldehyde continues the $\text{CH}_2\text{O} \rightarrow \text{HCO} \rightarrow \text{CO} \rightarrow \text{CO}_2$ reaction sequence with CO_2 as final product. As shown in Figure 3, MF seems to be an important intermediate in the total oxidation of DMM. In previous MF oxidation works, at atmospheric pressure²³ and higher pressures,¹⁶ the MF oxidation was seen to be initiated by its decomposition reaction to methanol (reaction 21). In this work, as an intermediate, MF is directly consumed by hydrogen abstraction reactions in order to produce CH_2OCHO and CH_3OCO radicals (reactions 22 and 23), with a relative importance, for example at 20 bar and oxidizing conditions ($\lambda = 20$), of 62% for reaction 22 and 20% for reaction 23.

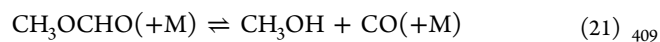
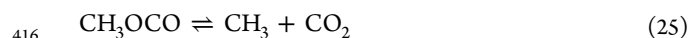
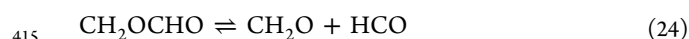


Table 3. Linear Sensitivity Coefficients for CO for Sets 1–9 in Table 1^a

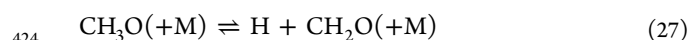
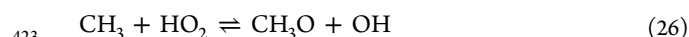
reaction	set 1 (623 K)	set 2 (623 K)	set 3 (573 K)	set 4 (673 K)	set 5 (623 K)	set 6 (523 K)	set 7 (548 K)	set 8 (548 K)	set 9 (548 K)
9 CH ₃ OCH ₂ OCH ₃ +OH=CH ₃ OCH ₂ OCH ₂ +H ₂ O	1.019	0.958	0.989	1.303	0.974	1.160	1.397	1.350	1.303
10 CH ₃ OCH ₂ OCH ₃ +OH=CH ₃ OCHOCH ₃ +H ₂ O	-0.219	-0.230	-0.352	-0.479	-0.251	-0.392	-0.487	-0.485	-0.479
11 CH ₃ OCH ₂ OCH ₃ +HO ₂ =CH ₃ OCH ₂ OCH ₂ +H ₂ O ₂	0.112	0.126	0.025	0.025	0.097	0.046	0.022	0.025	0.025
12 CH ₃ OCH ₂ OCH ₃ +HO ₂ =CH ₃ OCHOCH ₃ +H ₂ O ₂	0.126	0.124	0.022	0.033	0.087	0.086	0.035	0.036	0.033
14 CH ₃ OCH ₂ OCH ₃ +O ₂ =CH ₃ OCHOCH ₃ +HO ₂			0.001	0.001		0.017	0.007	0.003	0.001
16 CH ₃ OCH ₂ OCH ₂ +O ₂ =CH ₂ O+CH ₃ OCHO+OH	-0.184	-0.177	-0.216	-0.302	-0.182	-0.280	-0.322	-0.312	-0.302
19 CH ₃ OCH ₂ OCH ₂ +O ₂ (+M)=CH ₃ OCH ₂ O ₂ +CH ₂ O(+M)	0.179	0.174	0.214	0.301	0.179	0.279	0.317	0.309	0.301
CH ₃ OCH ₂ +O ₂ =CH ₂ O+CH ₂ O+OH	-0.021	-0.017	-0.008	-0.001	-0.017	-0.002	-0.001	-0.001	-0.001
CH ₂ OCH ₂ O ₂ H=CH ₂ O+CH ₂ O+OH	-1.479	-1.223	-0.705	-0.024	-1.164	-0.167	-0.075	-0.037	-0.024
CH ₃ OCH ₂ O ₂ =CH ₂ OCH ₂ O ₂ H	0.001	0.001	0.001	0.006	0.001	0.016	0.017	0.009	0.006
O ₂ CH ₂ OCH ₂ O ₂ H=CH ₂ OCH ₂ O ₂ H+O ₂	1.503	1.242	0.725	0.028	1.183	0.296	0.107	0.045	0.028
HO ₂ CH ₂ OCHO=OCH ₂ OCHO+OH	-0.028	-0.008	0.559	1.468	-0.006	1.659	1.795	1.614	1.468
CH ₃ OCHO+OH=CH ₂ OCHO+H ₂ O	0.071	0.059	0.023	-0.031	0.061	-0.054	-0.057	-0.044	-0.031
CH ₃ OCHO+OH=CH ₃ OCO+H ₂ O	0.002	0.004	-0.011	-0.021	0.004	-0.017	-0.023	-0.022	-0.021
CH ₂ OCHO+HO ₂ =HO ₂ CH ₂ OCHO	0.011	0.017	0.007	-0.010	0.017	-0.002	-0.007	-0.009	-0.010
H+O ₂ +N ₂ =HO ₂ +N ₂	-0.014	-0.010	-0.001	0.000	-0.005	0.000	0.000	0.000	0.000
OH+HO ₂ =H ₂ O+O ₂	-0.006	-0.005	-0.001	-0.002	-0.005	-0.002	-0.006	-0.003	-0.002
HO ₂ +HO ₂ =H ₂ O ₂ +O ₂	-0.160	-0.234	-0.056	-0.039	-0.192	-0.063	-0.026	-0.036	-0.039
H ₂ O ₂ +M=OH+OH+M	0.091	0.310	0.008	0.001	0.291	0.000	0.000	0.001	0.001
H ₂ O ₂ +OH=H ₂ O+HO ₂	-0.012	-0.030	-0.027	-0.025	-0.037	-0.002	-0.008	-0.017	-0.025
CH ₂ O+OH=HCO+H ₂ O	-0.851	-0.749	-0.608	-0.732	-0.735	-0.692	-0.811	-0.771	-0.732
CH ₂ O+HO ₂ =HCO+H ₂ O ₂	0.094	0.231	0.063	0.037	0.209	0.013	0.013	0.027	0.037
HCO+M=H+CO+M	0.014	0.009	0.003	0.000	0.004	0.001	0.000	0.000	0.000
HCO+O ₂ =HO ₂ +CO	-0.016	-0.012	0.095	0.001	-0.007	0.255	0.006	0.003	0.001

^aThe sensitivity coefficients are given as $A_i \delta Y_j / Y_j \delta A_i$, where A_i is the pre-exponential constant for reaction i and Y_j is the mass fraction of j th species. Therefore, the sensitivity coefficients listed can be interpreted as the relative change in predicted concentration for the species j caused by increasing the rate constant for reaction i by a factor of 2.

412 Both radicals decompose thermally, CH₂OCHO to give
413 formaldehyde and formyl radical and CH₃OCO to form methyl
414 radical and CO₂, through reactions 24 and 25, respectively:

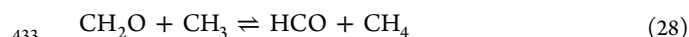


417 As reported in an earlier work by our group for methyl
418 formate oxidation,¹⁶ under high-pressure conditions, high
419 concentration of methyl and hydroperoxy radicals accumulate
420 and thus, the interaction of those radicals can generate methoxy
421 radicals through reaction 26, which further decomposes to
422 formaldehyde (reaction 27).



425 Therefore, formaldehyde is detected instead of methanol
426 (highly formed in both MF oxidation²³ and DMM oxidation¹⁵
427 at atmospheric pressure) when working under high pressure.

428 The formaldehyde obtained by this way continues the above-
429 mentioned CH₂O → HCO → CO → CO₂ reaction sequence.
430 A fraction of this formaldehyde reacts with methyl radicals
431 generating methane (reaction 28), which is detected as a final
432 product.



434 Figure 4 shows the influence of pressure on the DMM, CO₂,
435 CO, CH₂O and MF concentration profiles as a function of
436 temperature and for very oxidizing conditions, $\lambda = 20$. As
437 previously seen, working under high pressure conditions no
438 appreciable influence of pressure on the conversion regime of
439 DMM and products formation is found. Thus, similar results

have been obtained for 20, 40 and 60 bar, and the slight
differences that can be observed include a higher amount of
methyl formate for 20 bar, whereas for the other two values of
pressure, more CO₂ is produced. For the pressures of 40 and 60
bar, in the 598–673 K temperature range, a constant
concentration zone in the DMM profile and in the main
products, CO₂, CO, CH₃OCHO and CH₂O, can be observed.
This zone appears to be associated with the oxygenated
CH₃OCH₂O₂ species. In the mechanism taken as starting point
and used in the previous atmosphere work on DMM
conversion,¹⁵ the formation reactions of this species were not
included, and thus the predictions of the mechanism were
significantly worse. Therefore, the formation reactions of this
species from the interaction of CH₃OCH₂OCH₂ and O₂/HO₂
(active species under oxidizing and high pressure conditions),
reactions 19 and 20, were added to the mechanism.

With these two reactions, the current mechanism has been
able to represent the plateau observed in DMM, CO₂ and CO
concentration, in the 598–673 K temperature range. The
kinetic parameters of these reactions have been estimated due
to the lack of literature determinations above-mentioned, as has
been described in the Modeling section. Reaction pathway
analysis allows us to identify how the species are formed and
proceed through the following reaction sequence:
CH₃OCH₂O₂ → CH₂OCH₂O₂H → O₂CH₂OCH₂O₂H →
HO₂CH₂OCHO → OCH₂OCHO. The last one decomposes
to give CH₂O and HCOO through reaction 29:



Formaldehyde continues the CH₂O → HCO → CO → CO₂
well-known reaction sequence, whereas the hydrocarboxyl
radical decomposes generating CO₂ as a final product:



A first-order sensitivity analysis for CO has been performed for all the sets in Table 1. The results obtained, shown in Table 3, indicate that the conversion of DMM is highly sensitive to the DMM reactions with OH radicals (reactions 9 and 10), which have been previously discussed. Reactions involving MF (CH_3OCHO) and its radicals also present a high sensitivity, as an important intermediate in the DMM oxidation under the conditions studied in the present work.

Figure 5 shows the experimental results obtained for stoichiometric conditions by our research group for the

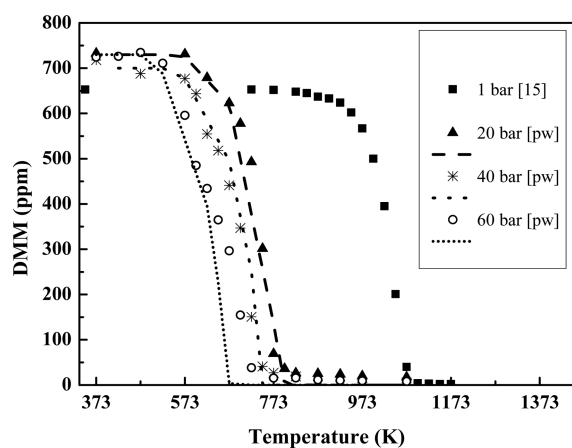


Figure 5. Results for stoichiometric conditions, at 1 bar (experimental) from Marrodán et al.¹⁵ and at high pressure (experimental and modeling) from the present work [pw], sets 4–6 in Table 1.

DMM oxidation at atmospheric pressure¹⁵ and the high-pressure results, experimental and modeling, discussed in the present work. Although it can be observed a huge shift to lower temperatures when moving from atmospheric pressure to higher ones, the results can not be directly compared because both gas residence times are significantly different. The gas residence time for the high pressure installation (t_r (s) = $261 \cdot P$ (bar)/ T (K)) is longer than at atmospheric pressure (t_r (s) = $195/T$ (K)) by a factor of 27–80 and, therefore, it is not possible to distinguish between the effect of pressure or residence time. To overcome this problem, model calculations have been carried out, modifying either the residence time or the pressure input value.

To do this, the kinetic mechanism used to simulate the high pressure experiments of this work has also been used to simulate the results obtained in the DMM oxidation at atmospheric pressure.¹⁵

Figure 6 shows, as an example, a comparison (only for DMM, CO and CO_2 concentrations) between the modeling results obtained with the initial mechanism¹⁵ (dashed lines) or with the mechanism modified in the present work (solid lines) and the experimental results (symbols) attained at atmospheric pressure in the 573–1373 K temperature range, for an initial concentration of 700 ppm of DMM and stoichiometric conditions.¹⁵ N_2 was used to achieve a total flow rate of 1000 mL (STP)/min, resulting in a gas residence time dependent on the reaction temperature of t_r (s) = $195/T$ (K).¹⁵ As can be seen in Figure 6, the modified mechanism generates almost the same results of the mechanism of reference¹⁵ and thus is able to

predict the main trends of the DMM consumption profile and CO and CO_2 formation.

With the validated kinetic mechanism of the present work, that describes well both low and high pressure experimental results, we have made different simulations to try to distinguish between the effect of residence time or pressure.

Figure 7 includes calculations for $\lambda = 1$ and 20 bar, with a residence time of t_r (s) = $5220/T$ (K) (solid lines) and for the same conditions ($\lambda = 1$ and 20 bar) but for a lower residence time of t_r (s) = $261/T$ (K) (short dashed lines), which would be the same as the residence time corresponding to 1 bar. As a reference, in Figure 7, also the experimental data of set 4 in Table 1 are included ($\lambda = 1, 20$ bar) and denoted by symbols. As can be seen, when only residence time is changed, increasing residence time shifts significantly the conversion of DMM toward lower temperatures.

Additionally, Figure 7 also includes calculations made with 1 bar of pressure and the residence time of the 20 bar experiments, i.e., t_r (s) = $5220/T$ (K) (long-dashed lines). Increasing pressure from 1 bar (long-dashed lines) to 20 bar (solid lines) but keeping a given residence time of t_r (s) = $5220/T$ (K) results in a similar shift of the DMM concentration profile as that reported for the change in time residence.

Thus, both the pressure and the residence time have an appreciable impact and are responsible for a significant shift in the oxidation regime of DMM.

CONCLUSIONS

The DMM conversion has been investigated in a quartz flow reactor in the 373–1073 K temperature range, for different air excess ratios ($\lambda = 0.7, 1$ and 20) and pressures (20–60 bar). The experimental results have been interpreted in terms of a detailed kinetic mechanism, compiled in a previous work about the DMM oxidation at atmospheric pressure by our research group,¹⁵ and modified in the present work to account also for the high pressure conditions studied. The modeling results obtained with the modified mechanism are similar to those attained without any modification; that is, the new mechanism is able to predict the main trends observed for the DMM oxidation at atmospheric pressure.

Experimental results and model calculations are, in general, in good agreement, and the main trends are well predicted for the theoretical model. Slight differences are noticed when working under stoichiometric or somewhat fuel-rich conditions, although the DMM conversion is a bit different for oxidizing conditions. Working at 20, 40 or 60 bar does not have a big effect on neither the oxidation of DMM nor the formation of the main products.

Independently of the conditions (stoichiometric, oxidizing or reducing), the main consumption of DMM occurs through H abstraction reactions by the hydroxyl radical (OH). Under oxidizing conditions, the conversion of DMM is fast until approximately the 598 to 673 K temperature zone, where the concentration of DMM presents a plateau and remains constant. This zone appears to be associated with the formation of the intermediate $\text{CH}_3\text{OCH}_2\text{O}_2$ oxygenated species. The formation reactions of this species from the interaction of $\text{CH}_3\text{OCH}_2\text{OCH}_2$ and O_2/HO_2 , active species under oxidizing and high pressure conditions, were not initially considered in the DMM reaction subset taken from the literature.¹⁴ Therefore, these reactions were added to the mechanism.

The analysis of the main reaction pathways involved in the DMM conversion, occurring under the conditions studied in

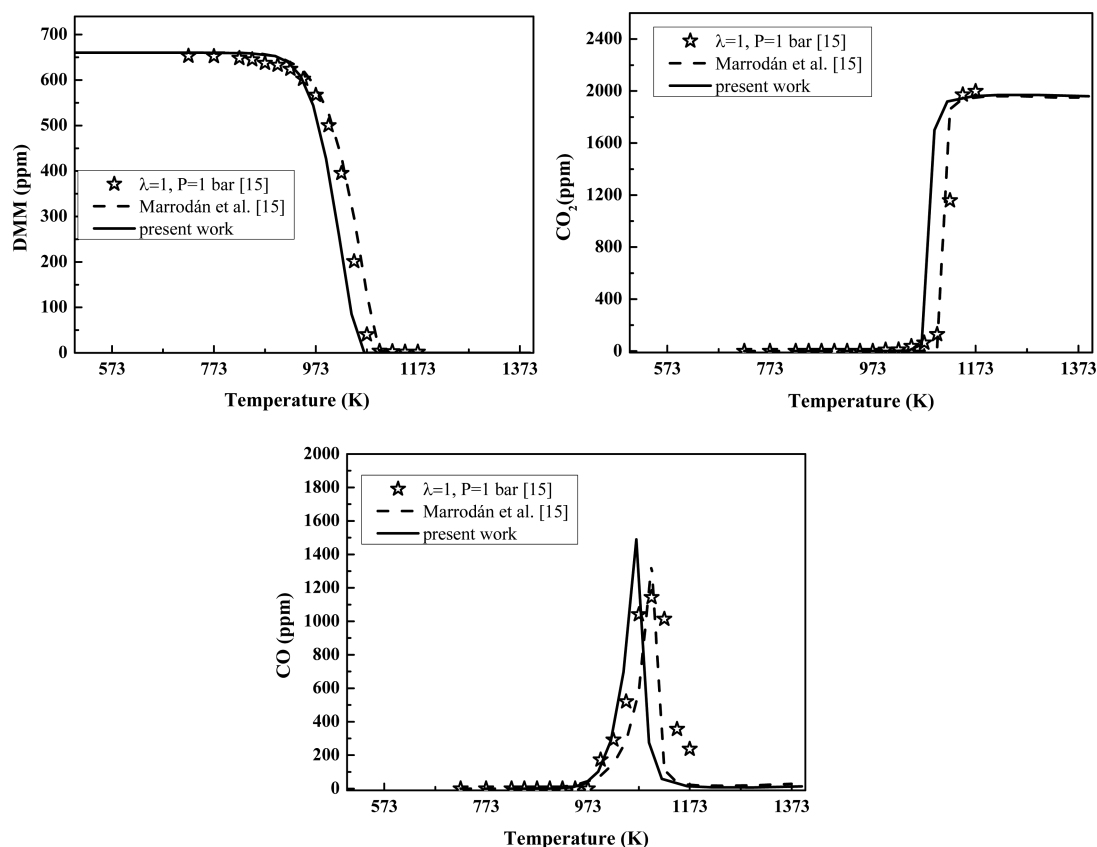


Figure 6. Comparison (for DMM, CO and CO₂ concentrations) between modeling calculations obtained with the initial mechanism¹⁵ and the mechanism used in the present work for the experimental results obtained at atmospheric pressure and $\lambda = 1$, for the conditions indicated in ref 15.

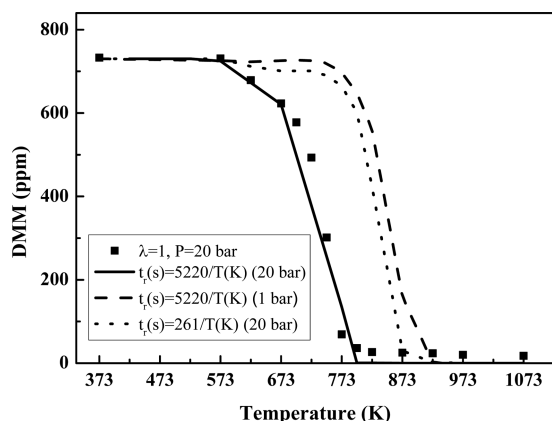


Figure 7. Evaluation through model calculations of the effect of gas residence time (comparison between solid lines, t_r (s) = 5220/ T (K), and short-dashed lines, t_r (s) = 261/ T (K)) and pressure (comparison between solid lines, t_r (s) = 5220/ T (K), and long-dashed lines, t_r (s) = 5220/ T (K)) for a selected example under the conditions indicated in set 4, Table 1.

573 the present work, has shown that methyl formate plays an
574 important role in this process.

575 The experimental results obtained under high-pressure
576 conditions in the present work are shifted toward lower
577 temperatures compared to those obtained at atmospheric
578 pressure by Marrodán et al.,¹⁵ for different residence times.
579 Model calculations have been performed to evaluate
580 independently the effect of pressure and gas residence time

and results indicate that both variables have remarkable
influence on the DMM oxidation process.

■ ASSOCIATED CONTENT

📄 Supporting Information

The full mechanism listing including the thermodynamic data additional to THERMDAT.⁴¹ The Supporting Information is available free of charge on the ACS Publications website at DOI: 10.1021/acs.energyfuels.5b00459.

■ AUTHOR INFORMATION

Corresponding Author

*M. U. Alzueta. E-mail: uxue@unizar.es.

Notes

The authors declare no competing financial interest.

■ ACKNOWLEDGMENTS

The authors express their gratitude to the Aragón Government (GPT group) and to MINECO and FEDER (Project CTQ2012-34423) for financial support.

■ REFERENCES

- (1) Zhu, R.; Wang, X.; Miao, H.; Yang, X.; Huang, Z. *Fuel* **2011**, *90*, 1731–1737.
- (2) Vertin, K. D.; Ohi, J. M.; Naegeli, D. W.; Childress, K. H.; Hagen, G. P.; McCarthy, C. I.; Cheng, A. S.; Dibble, R. W. *Methylal and Methylal-Diesel Blended Fuels for Use in Compression-Ignition Engines*; SAE Technical Paper 1999-01-1508; SAE International: Warrendale, PA, 1999.
- (3) Yanfeng, G.; Shenghua, L.; Hejun, G.; Tiegang, H.; Longbao, Z. *Appl. Therm. Eng.* **2007**, *27*, 202–207.

- 608 (4) Zhu, R.; Miao, H.; Wang, X.; Huang, Z. *Proc. Combust. Inst.* **2013**,
609 34, 3013–3020.
- 610 (5) Ren, Y.; Huang, Z.; Miao, H.; Di, Y.; Jiang, D.; Zeng, K.; Liu, B.;
611 Wang, X. *Fuel* **2008**, 87, 2691–2697.
- 612 (6) Ying, W.; Longbao, Z.; Hewu, W. *Atmos. Environ.* **2006**, 40,
613 2313–2320.
- 614 (7) Arcoumanis, C.; Bae, C.; Crookes, R.; Kinoshita, E. *Fuel* **2008**, 87,
615 1014–1030.
- 616 (8) Ren, Y.; Huang, Z.; Jiang, D.; Liu, L.; Zeng, K.; Liu, B.; Wang, X.
617 *Appl. Therm. Eng.* **2006**, 26, 327–337.
- 618 (9) Huang, Z. H.; Ren, Y.; Jiang, D. M.; Liu, L. X.; Zeng, K.; Liu, B.;
619 Wang, X. B. *Energy Convers. Manage.* **2006**, 47, 1402–1415.
- 620 (10) Sathiyagnanam, A. P.; Saravanan, C. G. *Fuel* **2008**, 87, 2281–
621 2285.
- 622 (11) Chen, G.; Yu, W.; Fu, J.; Mo, J.; Huang, Z.; Yang, J.; Wang, Z.;
623 Jin, H.; Qi, F. *Combust. Flame* **2012**, 159, 2324–2335.
- 624 (12) Zhang, C.; Li, P.; Li, Y.; He, J.; Li, X. *Energy Fuels* **2014**, 28,
625 4603–4610.
- 626 (13) Daly, C. A.; Simmie, J. M.; Dagaut, P.; Cathonnet, M. *Combust.*
627 *Flame* **2001**, 125, 1106–1117.
- 628 (14) Dias, V.; Lories, X.; Vandoooren, J. *Combust. Sci. Technol.* **2010**,
629 182, 350–364.
- 630 (15) Marrodán, L.; Monge, F.; Millera, A.; Bilbao, R.; Alzueta, M. U.
631 *Ninth Mediterranean Combustion Symposium*, Rhodes, Greece, June 7–
632 11, 2015, accepted for presentation.
- 633 (16) Marrodán, L.; Millera, A.; Bilbao, R.; Alzueta, M. U. *Energy Fuels*
634 **2014**, 28, 6107–6115.
- 635 (17) Glarborg, P.; Alzueta, M. U.; Dam-Johansen, K.; Miller, J. A.
636 *Combust. Flame* **1998**, 115, 1–27.
- 637 (18) Glarborg, P.; Alzueta, M. U.; Kjærgaard, K.; Dam-Johansen, K.
638 *Combust. Flame* **2003**, 132, 629–638.
- 639 (19) Skjøth-Rasmussen, M. S.; Glarborg, P.; Østberg, M.;
640 Johannessen, J. T.; Livbjerg, H.; Jensen, A. D.; Christensen, T. S.
641 *Combust. Flame* **2004**, 136, 91–128.
- 642 (20) Alzueta, M. U.; Muro, J.; Bilbao, R.; Glarborg, P. *Isr. J. Chem.*
643 **1999**, 39, 73–86.
- 644 (21) Alzueta, M. U.; Hernández, J. M. *Energy Fuels* **2002**, 16, 166–
645 171.
- 646 (22) Alzueta, M. U.; Borruey, M.; Callejas, A.; Millera, A.; Bilbao, R.
647 *Combust. Flame* **2008**, 152, 377–386.
- 648 (23) Alzueta, M. U.; Aranda, V.; Monge, F.; Millera, A.; Bilbao, R.
649 *Combust. Flame* **2013**, 160, 853–860.
- 650 (24) Dagaut, P.; Boettner, J. C.; Cathonnet, M. *Proc. Combust. Inst.*
651 **1996**, 26, 627–632.
- 652 (25) Mallard, W. G.; Westley, F.; Herron, J. T.; Hampson, R. F. *NIST*
653 *Chemical Kinetics Database*, version 6.01, 1994.
- 654 (26) Foucaut, J. F.; Martin, R. *J. Chim. Phys.* **1978**, 75, 132–144.
- 655 (27) Dean, A. M. *J. Phys. Chem.* **1985**, 89, 4600–4608.
- 656 (28) Dagaut, P.; Daly, C.; Simmie, J. M.; Cathonnet, M. *Proc.*
657 *Combust. Inst.* **1998**, 27, 361–369.
- 658 (29) Faubel, C.; Hoyermann, K.; Strofer, E.; Wagner, H. *Ber.*
659 *Bunsenges Phys. Chem.* **1979**, 83, 532–538.
- 660 (30) Herron, J. T. *J. Phys. Chem. Ref. Data* **1988**, 17, 967–1026.
- 661 (31) Arif, M.; Dellinger, B.; Taylor, P. H. *J. Phys. Chem. A* **1997**, 101,
662 2436–2441.
- 663 (32) DeMore, W. B.; Bayes, K. D. *J. Phys. Chem. A* **1999**, 103, 2649–
664 2654.
- 665 (33) Cook, R. D.; Davidson, D. F.; Hanson, R. K. *J. Phys. Chem. A*
666 **2009**, 113, 9974–9980.
- 667 (34) Curran, H. J.; Pitz, W. J.; Westbrook, C. K.; Dagaut, P.;
668 Boettner, J. C.; Cathonnet, M. *Int. J. Chem. Kinet.* **1998**, 30, 229–241.
- 669 (35) Sehested, J.; Sehested, K.; Platz, J.; Egsgaard, H.; Nielsen, O. J.
670 *Int. J. Chem. Kinet.* **1997**, 29, 627–637.
- 671 (36) Sehested, J.; Mogelberg, T.; Wallington, T. J.; Kaiser, E. W.;
672 Nielsen, O. J. *J. Phys. Chem.* **1996**, 100, 17218–17225.
- 673 (37) Hoyerman, K.; Nacke, F. *Proc. Combust. Inst.* **1996**, 26, 505–
674 512.
- 675 (38) Lutz, A. E.; Kee, R. J.; Miller, J. A. *SENKIN: A FORTRAN*
676 *Program for Predicting Homogeneous Gas Phase Chemical Kinetics with*
Sensitivity Analysis; Sandia National Laboratories: Livermore, CA, 677
1988; Report SAND87-8248. 685
(39) Kee, R. J.; Rupley, F. M.; Miller, J. A. *CHEMKIN-II: A 679*
FORTRAN Chemical Kinetics Package for the Analysis of Gas-Phase 680
Chemical Kinetics; Sandia National Laboratories: Albuquerque, NM, 681
1991; Report SAND87-8215. 682
(40) *CHEMKIN-PRO*, Release 15131; Reaction Design: San Diego, 683
2013. 684
(41) Burcat, A.; Ruscic, B. *Third Millennium Ideal Gas and Condensed 685*
Phase Thermochemical Database for Combustion with Updates from 686
Active Thermochemical Tables; Report TAE960; Technion Israel 687
Institute of Technology: Haifa, Israel, 2005. 688